International Journal of GEOMATE, March, 2017, Vol. 12, Issue 31, pp. 71-76
Geotec., Const. Mat. & Env., ISSN:2186-2990, Japan, DOI: http://dx.doi.org/10.21660/2017.31.6547

EVALUATION OF POROSITY IN BIOGROUTED SAND USING MICROFOCUS X-RAY CT

*Shumpei Mitsuyama[1] , Kazunori Nakashima[2], Satoru Kawasaki[2]

[1]Graduate School of Engineering, Hokkaido University, Sapporo, Japan
[2]Faculty of Engineering, Hokkaido University, Sapporo, Japan

*Corresponding Author, Received: 9 June 2016, Revised: 10 August 2016, Accepted: 30 Nov. 2016

ABSTRACT: Biogrouting is a method employed for ground improvement based on microbially induced calcium carbonate precipitation. It is commonly believed that biogrout has environmental and economic benefits. However, there remains the need to clearly understand the internal structure of biogrouted soil. In this study, we use microfocus X-ray computed tomography (CT) to evaluate the porosity in biogrouted sand. X-ray CT is useful as a non-distractive inspection tool. First, we prepare small specimens using coral sand at different dilution rates of culture solution. After carrying out a solidification test for 2 wks., we perform an unconfined compressive strength (UCS) test and measure the porosity of the specimens. Our aim is to investigate the influence of the dilution rate on the UCS and the porosity of sand specimens. The results show that a lower dilution rate resulted in a lower sand-specimen porosity and an increase in the UCS. We investigate the precipitation that fills a void. Then, we investigate the relationship between UCS and the ratio of porosity. There was a negative correlation between UCS and porosity, which closely agrees with previous research. We confirm the validity of the result, and we determine the UCS from the porosity.

Keywords: Sand Solidification, X-ray CT, Ureolytic Bacteria

1. INTRODUCTION

Recently, artificial beachrock obtained by biogrout solidification through microbially induced carbonate precipitation (MICP) [1]–[5] has attracted a great deal of attention. This method can be applied to ground improvement and coastal protection[6]–[8], and it is believed that it is environmentally friendly and low cost. In previous studies, precipitation in sand specimens was evaluated by measuring the unconfined compressive strength (UCS). However, the amount of precipitation varies depending on the location [9]. Understanding the internal quantity of calcium carbonate is key to improve the UCS. In this study, we determine experimentally the porosity, which indicates the proportion of pores in the total volume in the specimen. There are several ways to measure the porosity, including the mercury intrusion technique and the liquid saturation method [10]. However, these methods result in the deformation of internal structures. In this study, we evaluate the porosity using microfocus X-ray computed tomography (CT). X-ray CTs can visualize the internal structure quantitatively without any deformation. Therefore, UCS and porosity can be measured using the same sample.

As shown in Fig. 1, Microbial urease catalyzes the hydrolysis of urea into ammonium and carbon dioxide (Eqs. (1) and (2)).

$$\mathbf{CO(NH_2)_2 + 3H_2O \rightarrow 2NH_4^+ + 2OH^- + CO_2} \quad (1)$$

$$\mathbf{CO_2 + H_2O \rightarrow HCO_3^- + H^+} \quad (2)$$

The carbonate ions react with calcium ions. Then, calcium carbonate precipitates between sand grains and form cementing bonds (Eq. (3)).

$$\mathbf{Ca^{2+} + HCO_3^- + OH^- \rightarrow CaCO_3 + H_2O} \quad (3)$$

The byproduct, which is the ammonium ion, can result in an increased pH. The precipitation of calcium carbonate tends to take place at higher pH values.

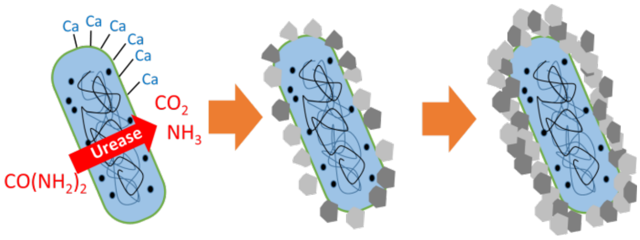

Fig. 1 Urea hydorolysis reaction.

2. METHOD

We used *Pararhodobacter* sp., which was isolated from the beach sand in Sumuide, Nago, Okinawa, Japan [11]. The grain size is shown in Fig. 2. We obtained 1 g of bacteria cultivated on ZoBell 2216E plate medium (polypeptone 5.0 g/L, yeast extract 1.0 g, and $FePO_4$ 0.1 g/L with artificial seawater) for 72 h and placed it in 100 mL of ZoBell medium solution. Then, we shook it at 30°C, 160 rpm for 24 h. In the meanwhile, 40 g of coral sand was dried at 110°C for 24h.

Table 1 Composition of cementation solution (solvent: artificial seawater).

Reagent	Content (g / L)
Nutrient broth	3.00
NH_4Cl	10.00
$NaHCO_3$	2.12
$CO(NH_2)_2$	30.00
$CaCl_2$	55.5

We separated the cells by centrifugation at 30°C, 3000 rpm for 10 min. We extracted 10 mL at the bottom and moved it to a 90 mL ZoBell 2216E medium. We shook it at 30°C, 160 rpm for 24 h again. As indicated in Fig. 3, we set the syringes at 30°C in an incubator. On the first day, we diluted the culture solution with ZoBell 2216E medium. Sixteen mL of culture medium solution and 20 mL of the cementation solution as shown in Table 1 were added to each syringe. The test conditions of the syringe test are shown in Table 2. Then, we injected 20 mL of cementation solution and drained every 24 h for 2 wks. We measured the pH and concentration of Ca^{2+} every 3 d. At the end of the experiment, we drained all of the solution in the specimens.

We also measured the needle-penetration inclination (diameter = 2.5 cm, height = 7 cm). The UCS was estimated using a needle penetration device (SH-70, Maruto Testing Machine Company, Tokyo, Japan). Equation (4) describes the relationship between the UCS (y) and the needle penetration inclination (x) determined from 114 natural rock samples and 50 improved soils with cement.

$$\log(y) = 0.978\log(x) + 2.621 \qquad (4)$$

In addition, we observed samples using a microfocus X-ray CT. After performing the solidification test for 2 wks., we also measured the porosity in order to investigate the influence of the dilution rate on the UCS and the porosity of sand specimens. In the X-ray CT images, the smallest unit is called a voxel [12]. A voxel has a CT value as given in Eq. (5).

$$\text{CT value} = S\mu + B \qquad (5)$$

S is the slope, B is the bias and μ is attenuation coefficients of X-ray beams. In this study, S = 200 and B = 0. The voxel size is 25 μm ×25 μm × 40 μm. In the experiment, we obtained 80 slice images using a TOSCANER 31300 μhd (Toshiba IT & Control Systems Co., Ltd.), which is installed at Hokkaido University, Japan. The applied tube voltage was 130 kV, and the maximum tube current was 62 μA. In this experiment, we used the cone-beam scanning mode, and the number of pixels was 1024 × 1024. Using the maximum-likelihood thresholding method [10], we then determined the threshold to measure the porosity.

Table 2 Test conditions for syringe tests.

Case number	Dilution rate
Case 1	1
Case 2	2
Case 3	5
Case 4	10

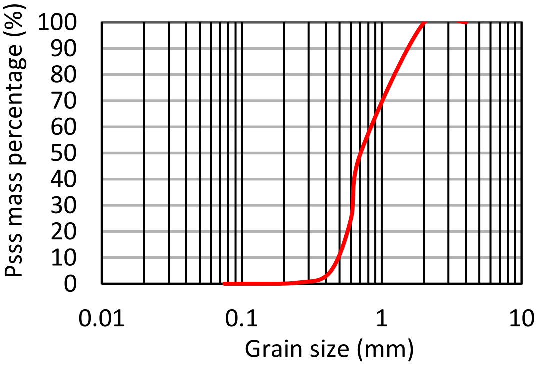

Fig. 2 Grain size distribution of coral sand.

Fig. 3 Syringe cementation test.

3. RESULTS

The sand was cemented, as shown in Fig. 4, and as shown in Fig. 5, the UCS increase as the dilution rates decrease. One explanation for this is that the UCS is related to the number of bacteria. Moreover, the sand in Case 4 was cemented only at the surface (2-cm thick). For cases 1 and 2, the estimated UCS value tended to be higher than in cases 3 and 4. For case 1, the UCS at the upper edge is a maximum of 7 MPa. For case 4, the UCS at the bottom edge is 0 MPa. This point was not solidified. The bottom UCS is markedly low since the amount of bacteria is sufficiently small. In addition, we estimated the amount of CaCO$_3$ in the sand based on the Ca^{2+} concentration of the drainage at 3, 6, 9, 12, and 14 d. From Fig. 6, the amount of CaCO$_3$ increased for all cases with time. However, the slope of Case 1 on the graph is highest. The amount of CaCO$_3$ tended to rise significantly when we used dilution rates of 1 and 2. We also measured the pH at the drainage. As shown in Fig. 7, the pH decreases with time. From the above, the amount of bacteria decreased with time. Fig. 8 shows X-ray CT images of all cases. The brighter areas represent higher density regions, while the darker areas represent lower density regions. Further, the porosity values for all cases are shown in Table 3. The results clarified that a lower dilution rate results in a decreased porosity of the sand specimen and an increase in the UCS.

Fig. 4 Syringe specimen of Case 1 after 14 d of curing.

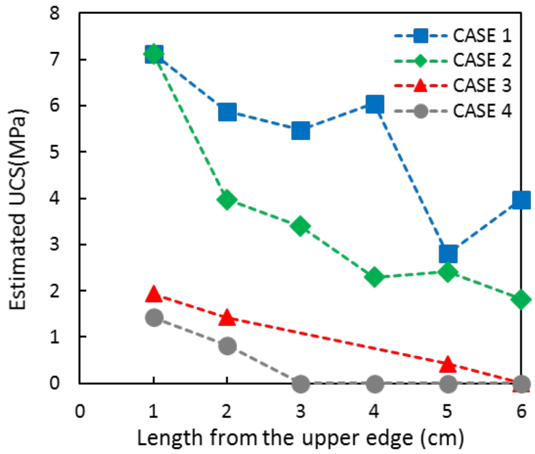

Fig. 5 The UCS of each specimen

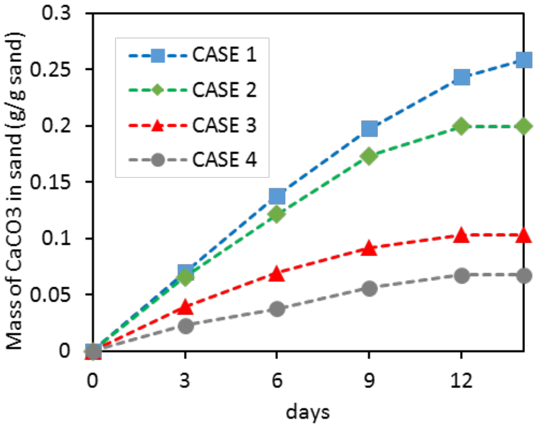

Fig.6 The amount of CaCO$_3$

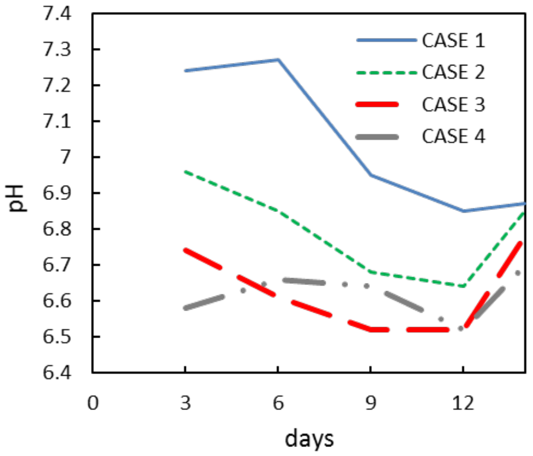

Fig.7 Variation in the pH values of drainage.

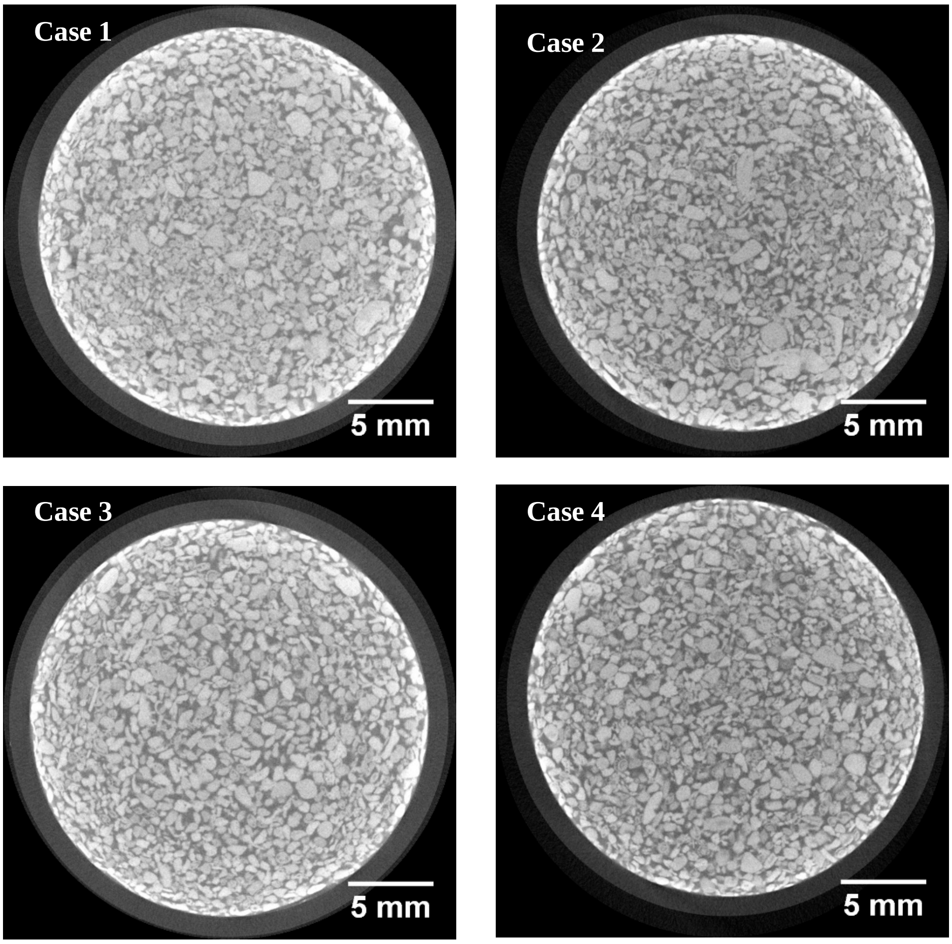

Fig. 8 X-ray CT images at the upper edge.

Table 3 The porosity based on the syringe test.

Case number	Porosity at the upper edge (%)	Porosity at the bottom edge (%)
without bacteria	42.9	50.6
Case 1	31.0	32.7
Case 2	31.8	34.8
Case 3	31.6	40.0
Case 4	33.0	39.6

4. DISCUSSION

As shown in Fig. 9, there is a relationship between the porosity (n) and UCS (q_u) (Eq. (6)) (correlation coefficient: 0.5956).

$$q_u = -0.6092\, n + 23.787 \ (R^2 = 0.5956) \qquad (6)$$

There is a negative correlation between UCS and the porosity. This negative correlation closely agrees with previous research. Miyagi and Komiya [13] reported the relationship between UCS and porosity (Eq. (7)) (correlation coefficient: 0.291) of natural sandy limestone in Okinawa, Japan.

$$q_u = -0.7616\, n + 30.55 \ (R^2 = 0.291) \qquad (7)$$

The porosity and UCS is found to be smaller than the values for natural beachrock. From this graph, if all voids are filled with precipitation, the strength will increase to 23.8 MPa. In the case where the porosity is greater than 39.0%, the specimen is not solidified. For the same porosity, UCS is different, and this is because the initial porosity is different. The number of samples is low, and more samples are therefore needed.

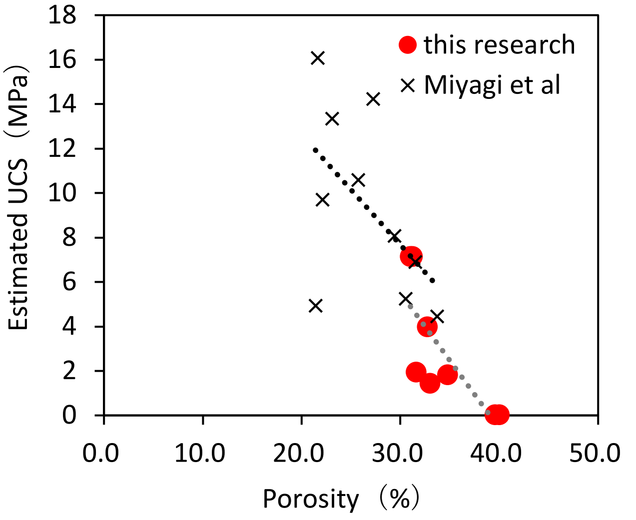

Fig. 9 Relation ship between Estimated UCS and Porosity

5. CONCLUSION

In this study, we cemented sand specimens using different dilution rates with a culture solution to determine the effects of various conditions on the USC and porosity. The main findings of this study are as follows:

(1) The sand specimens were cemented up to 7 MPa after 14 d using one dilution rate. The lower dilution rate is, the higher UCS is.
(2) We observed the filling of the pore with precipitation.
(3) There is a negative correlation between UCS and porosity.

6. REFERENCES

[1] A. Al Qabany, K. Soga *et al.*, “Factors Affecting Efficiency of Microbially Induced Calcite Precipitation,” Jounal Geotech. geoenvironmental Eng., Vol. 138, No. 8, pp. 992–1001, 2012.

[2] L. A. Van Paassen, R. Ghose *et al.*, “Quantifying Biomediated Ground Improvement by Ureolysis : Large-Scale Biogrout Experiment,” Jounal Geotech. geoenvironmental Eng., Vol. 136, No. 12, pp. 1721–1728, 2010.

[3] V. Achal and S. Kawasaki, “Biogrout : A Novel Binding Material for Soil Improvement and Concrete Repair,” Front. Microbiol., Vol. 7, No. 3, pp. 9–11, 2016.

[4] M. Li, Q. Fu *et al.*, “Bio-grout based on microbially induced sand solidification by means of asparaginase activity,” Sci. Rep., Vol. 5, pp. 1–9, 2015.

[5] J. T. Dejong, M. B. Fritzges *et al.*, “Microbially Induced Cementation to Control Sand Response to Undrained Shear,” Jounal Geotech. geoenvironmental Eng., Vol. 132, no. 12, pp. 1381–1392, 2006.

[6] T. Danjo and S. Kawasaki, “Microbially Induced Sand Cementation Method Using Pararhodobacter sp Strain SO1, Inspired by Beachrock Formation Mechanism,” Min. Mater. Process. Inst. Japan, No. 1, 2016.

[7] T. Danjo and S. Kawasaki, “A Study of The Formation Mechanism of Beachrock in Okinawa, Japan: Toward Making artificial Rock,” Int. J. GEOMATE, Vol. 5, No. 1, pp. 634–639, 2013.

[8] M. Nakibul H. Khan, S. Shimazaki *et al.*, “Coral Sand Solidification Test Through Miceobial Calcium Carbonate Precipitation Using Pararhodobacter sp.,” Int. J. GEOMATE, Vol. 11, No. 26, pp. 2665–2670, 2016.

[9] V. S. Whiffin, L. A. van Paassen *et al.*, “Microbial Carbonate Precipitation as a Soil Improvement Technique,” Geomicrobiol. J., Vol. 24, No. 5, pp. 417–423, 2007.

[10]M. Kato, M. Takahashi *et al.*, “Evaluation of Porosity and Its Variation in Porous Materials Using Microfocus X-ray Computed Tomography Considering the Partial Volume Effect,” Mater. Trans., Vol. 54, No. 9, pp. 1678–1685, 2013.
[11]Takashi Danjo, “Fundamental study on development of artificial rock learnt from beachrock formation mechanism,” Grad. Sch. Eng. Dr. Thesis, 2015.
[12]H. Yamanaka, Satoru Kawasaki *et al.*, “Segmentation of internal structure of two-phase materials using micro-focus X-ray CT,” Japanese Geotech. J., Vol. 6, No. 2, pp. 273–284, 2011.
[13]N. Miyagi and Y. Komiya, “Effective porosity and compression strength of Ryukyu limestone in Pleistocene Epoch in the Quanternary period,” Univ. Ryuku A